A novel analytical solution to steady-state evaporation from porous media

Morteza Sadeghi,[1,2] Nima Shokri,[3] and Scott B. Jones[1]

[1]   Evaporation from soil and other porous media constitutes a significant source of water loss affecting global water balance and energy exchange between land and atmosphere. The presence of a shallow water table can lead to sustained water loss that is dependent on porous media hydraulic properties and water table depth among other factors. In this paper, an exact analytical solution to steady state evaporation from porous media is developed using the Brooks-Corey hydraulic conductivity model. The solution is presented in terms of a set of infinite series. An advantage of this solution compared to previous derivations is that the infinite series can be very closely approximated using a closed-form solution (i.e., excluding integrals or series). The novel solution shows excellent agreement with the exact solution for a broad range of soil texture from sand to clay. The applicability of the solution to predict the location of the drying front was also verified using experimental data taken from the literature. The solution may be used for directly modeling steady state evaporation or for inverse determination of the Brooks-Corey hydraulic parameters.

1.   Introduction

1.1.   Steady-State Evaporation in the Presence of a Water Table

[2]   Steady state evaporation from a fixed water table (WT) or groundwater level may be considered using two general cases [*Gowing et al.*, 2006; *Lehmann et al.*, 2008; *Shokri and Salvucci*, 2011]. In the first case, the water table depth, D, is shallow enough to maintain the hydraulic connections between the WT and the surface via capillary induced liquid flow. For this case, water in a liquid state flows through the entire profile and vaporizes at the surface. The maximum WT depth, down to which the hydraulic connection is maintained, D_{max}, depends on the porous medium properties and on the evaporation rate, which in this case is close to the atmospheric demand or evaporation rate from a saturated surface.

[3]   The second case applies when the WT lies below D_{max} (i.e., $D > D_{max}$) indicating hydraulic disconnection between the WT and the surface due to the limiting effects of downward gravity and viscosity forces. This results in the evolution of the vaporization plane from the surface to an intermediate depth between the surface and the WT referred to as "drying front" (DF) marking the interface between dry

and partially saturated zone. Therefore, three distinct zones are formed along the profile above the WT: a saturated zone or liquid region known as capillary fringe, an intermediate transition zone termed the "film region" [*Yiotis et al.*, 2003] between the capillary fringe and DF, and a near surface dry zone (gas region) above the DF (Figure 1). In this case, liquid water flows through liquid and film regions, vaporizes at the DF and moves in the gas phase toward the surface by diffusion [*Shokri and Salvucci*, 2011].

[4]   The soil-water pressure head distribution, $h(z)$, along the liquid and film regions may be modeled using Darcy's law:

$$e = K(h)\left(\frac{dh}{dz} - 1\right) \tag{1}$$

where h (m) is the pressure head (absolute value), z (m) is the vertical distance from the WT (positive upward), e (m s^{-1}) is the steady state evaporation rate, and $K(h)$ (m s^{-1}) is the unsaturated hydraulic conductivity function.

[5]   When the WT depth is greater than D_{max}, the location of the DF will be where K approaches 0 and as a result dh/dz approaches infinity to keep e constant. Hence, h increases sharply over a very short vertical distance until reaches a critical pressure head, h_{DF}, at the DF. Such an increase in h results in an abrupt change in soil water content, which is related to h through the so-called soil-water retention function. Therefore, the hydraulic disruption and the phase change occur at the DF. Within the gas region, h varies from h_{DF} to a limiting pressure head at the surface that is equal to the atmospheric pressure head [*Edelfsen and Anderson*, 1943] as

$$h_{atm} = \frac{RT}{Mg}|\ln H_r| \tag{2}$$

---

[1]Department of Plants, Soils and Climate, Utah State University, Logan, Utah, USA.
[2]Department of Water Engineering, Ferdowsi University of Mashhad, Mashhad, Iran.
[3]Department of Earth and Environment, Boston University, Boston, Massachusetts, USA.

Corresponding author: M. Sadeghi, Department of Plants, Soils, and Climate, Utah State University, Logan, UT 84322, USA. (scott.jones@usu.edu)
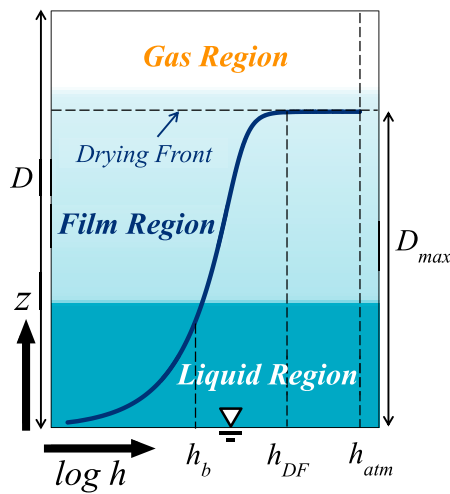
Figure 1. Graphical description of the three regions modeled for steady state evaporation. Pressure head distribution (absolute value) along the liquid and film regions is modeled using Darcy's law.

where T (K) is the air temperature near the surface, g is the acceleration due to gravity (9.81 m s^{-2}), M the molecular weight of water (0.01802 kg mol^{-1}), R is the universal gas constant (8.3143 kg m^2 s^{-2} mol^{-1} K^{-1}) and H_r is the relative humidity of air. For most weather conditions, h_{atm} is large enough (greater than 1000 m) to fully dry most soils.

[6] Figure 1 graphically shows the three aforementioned regions and a schematic solution for Darcy's law along the liquid and film regions (the curve within the liquid and film regions shows the h distribution on a logarithmic scale). Experimental results indicate that in the gas region, h is close to h_{atm} [*Gowing et al.*, 2006]. As discussed by *Shokri and Salvucci* [2011], due to the absence of liquid continuity through the gas layer, Darcy's law cannot be applied through the entire profile for calculation of the liquid flux. In such cases, liquid water is transported to the drying front via capillary induced liquid flow followed by liquid vaporization at the drying front and vapor diffusion through the overlying dry layer. Thus, Fickian diffusion law may be used to calculate the diffusive flux considering the gradient of vapor pressure between the DF and the surface [*Gardner*, 1958; *Shokri et al.*, 2009]. However, in the case of a steady state process, the Darcy flux below the DF will be equal to the vapor diffusion flux above the DF, where both are equal to the steady state evaporation rate (conservation of mass).

1.2. Literature Review

[7] Analytical solutions for Darcy's law for steady state evaporation from soil have been developed mainly for the $K(h)$ functions of *Gardner* [1958]:

$$K = \frac{K_s}{1 + (h/h_b)^P} \qquad (3)$$

and *Brooks and Corey* [1964]:

$$K = \begin{cases} K_s & (h \le h_b) \\ K_s(h/h_b)^{-P} & (h > h_b) \end{cases} \qquad (4)$$

where K_s is the saturated hydraulic conductivity, h_b is the bubbling pressure head, and P is a shape parameter. The bubbling pressure head, h_b, is the minimum pressure head required to drain or invade the largest soil pore upon desaturation. *Gardner* [1958] developed a solution for the $K(h)$ function of equation (3) adopting $P = 1$, 1.5, 2, 3, and 4. For all noninteger $P > 1$, *Warrick* [1988] developed exact solutions for both functions of (3) and (4). The solutions were obtained for $z(h, e)$ in terms of an incomplete Beta function (an integral function) and a hypergeometric function (an infinite series). To introduce the more desirable solutions of $h(z, e)$ and $e(z, h)$, *Salvucci* [1993] introduced closed-form approximate solutions for the case of the Gardner function, equation (3). The approximate solutions agreed reasonably well with numerical solutions for coarse-textured soils but introduced deviations for fine-textured soils.

[8] *Shokri and Salvucci* [2011] argued that the aforementioned solutions overlooked the discontinuity at the DF by applying Darcy's law to the entire soil profile. To solve for the maximum height of liquid continuity above the WT, $D_{\max}$, they alternatively applied an approximate solution to Darcy's law following *Lehmann et al.* [2008]. In their solution, the drying front pressure head, h_{DF}, was found by linearization of the soil-water retention curve using its central slope (i.e., assuming that the soil-water content decreases linearly by increasing h). Subsequently, the pressure head gradient along the liquid and film regions was modeled using Darcy's law by assigning an average K. They showed the method provides better predictions for coarse-textured soils compared to fine-textured soils, where the underlying assumptions (i.e., water retention linearization and K averaging) may be less applicable.

[9] In this study, by applying the Brooks-Corey hydraulic conductivity function, we develop an exact solution to Darcy's law to model the h distribution along the liquid and film regions and to offer a new analytical tool to predict $D_{\max}$. The solutions are presented in terms of a set of infinite series, allowing consideration of the phase discontinuity. An additional advantage of this solution compared to that of *Warrick* [1988] is that the infinite series can be very closely approximated using a closed-form solution (i.e., excluding integrals or series). Such solutions are more easily applied, for example for inverse fitting soil hydraulic properties from evaporation experiments.

2. New Solution

[10] Applying the Brooks-Corey function, equation (4), to Darcy law, equation (1), yields:

$$z = \begin{cases} (1+r)^{-1}h & (h \le h_b) \\ (1+r)^{-1}h_b + \displaystyle\int_{h_b}^{h} \frac{K(h)}{K(h)+e} dh & (h_b < h \le h_{DF}) \end{cases} \qquad (5)$$

where $r = e/K_s$. For cases with $e < K_s$, we define the following variables:

$$T(h) = -\frac{e}{K(h)} = -r\left(\frac{h}{h_b}\right)^P \qquad (h_b < h \le h_e) \qquad (6a)$$

$$U(h) = -\frac{K(h)}{e} = -\frac{1}{r}\left(\frac{h}{h_b}\right)^{-P} \qquad (h_e < h \le h_{DF}) \qquad (6b)$$

where h_e is the pressure head at which $e = K(h)$ or:

$$h_e = h_b r^{-1/P} \tag{7}$$

Equation (6) gives:

$$
\begin{aligned}
I &= \int_{h_b}^{h} \frac{K(h)}{K(h) + e} dh \\
&= \begin{cases}
\displaystyle\int_{h_b}^{h} \frac{dh}{1 - T(h)} & (h_b < h \leq h_e) \\
\displaystyle\int_{h_b}^{h_e} \frac{dh}{1 - T(h)} + \int_{h_e}^{h} \frac{-U(h)dh}{1 - U(h)} & (h_e < h \leq h_{DF})
\end{cases}
\end{aligned} \tag{8}
$$

[11] Since $e < K_s$, the absolute values of T and U are less than unity. Hence, a Maclaurin series expansion for $|x| < 1$ written as $(1 - x)^{-1} = 1 + x + x^2 + x^3 + \ldots$ can be applied to equation (8) yielding:

$$
I = \begin{cases}
\displaystyle\int_{h_b}^{h} \left(1 + T + T^2 + \ldots\right) dh & (h_b < h \leq h_e) \\
\displaystyle\int_{h_b}^{h_e} \left(1 + T + T^2 + \ldots\right) dh - \int_{h_e}^{h} \left(U + U^2 + U^3 + \ldots\right) dh & (h_e < h \leq h_{DF})
\end{cases} \tag{9}
$$

[12] Combining equations (6) and (9) and a term-by-term solution of the integral I, followed by substitution into equation (5), gives an exact solution to equation (1) as follows:

$$
z = \begin{cases}
(1 + r)^{-1} h & (h \leq h_b) \\
\displaystyle(1 + r)^{-1} h_b + h_e \sum_{i=0}^{\infty} \frac{(-1)^i (h/h_e)^{1+iP}}{1 + iP} - h_e \sum_{i=0}^{\infty} \frac{(-1)^i (h_b/h_e)^{1+iP}}{1 + iP} & (h_b < h \leq h_e) \\
\displaystyle z(h_e) + h_e \sum_{i=1}^{\infty} \frac{(-1)^{i+1} (h/h_e)^{1-iP}}{1 - iP} - h_e \sum_{i=1}^{\infty} \frac{(-1)^{i+1}}{1 - iP} & (h_e < h \leq h_{DF})
\end{cases} \tag{10}
$$

[13] The series converge rapidly (i.e., within the first few terms) to the exact solution of the problem. The convergence is more rapid for coarser textured soils in which the $K(h)$ function more rapidly approaches zero. As demonstrated in Appendix A, an excellent approximation of equation (10) is found in the following closed-form solution:

$$
z = \begin{cases}
(1 + r)^{-1} h & (h \leq h_b) \\
z_1 + h - (1 + P)^{-1} h \ln\left[1 + r(h/h_b)^P\right] & (h_b < h \leq h_e) \\
z_2 + (1 - P)^{-1} h \ln\left[1 + r^{-1}(h/h_b)^{-P}\right] & (h_e < h \leq h_{DF})
\end{cases} \tag{11}
$$

where:

$$z_1 = h_b \left[\frac{\ln(1 + r)}{1 + P} - \frac{r}{1 + r}\right] \tag{12}$$

$$
z_2 = h_b \left\{ \frac{\ln(1 + r)}{1 + P} - \frac{r}{1 + r} - r^{-1/P} \right. \\
\left. \cdot \left[\frac{\ln 2}{(1 - P)} + \frac{\pi^2/12 - \ln 2}{P(1 - P)} - 1 + \frac{\ln 2}{1 + P}\right] \right\} \tag{13}
$$

[14] Since $K(h_{DF}) = K_s(h_{DF}/h_b)^{-P}$ is practically zero, $D_{\max} = z(h_{DF})$ is practically equal to z_2 in equation (13). Note that z_2 is equivalent to d in equation (26) of *Warrick* [1988] and is realized when $h \to \infty$. Although z_2 (or d of Warrick) is practically equal to $D_{\max}$, in theory, z_2 extends slightly beyond the drying front into the gas region (see Figure 1).

[15] Equations (10) and (11) are applicable when $e < K_s$. For cases with $e \geq K_s$, a similar approach yields the following solution:

$$
z = \begin{cases}
(1 + r)^{-1} h & (h \leq h_b) \\
z_3 + (1 - P)^{-1} h \ln\left[1 + r^{-1}(h/h_b)^{-P}\right] & (h_b < h \leq h_{DF})
\end{cases} \tag{14}
$$

where:

$$z_3 = h_b \left[\frac{\ln(1 + 1/r)}{P - 1} + \frac{1}{1 + r}\right] \tag{15}$$

[16] In this case, $D_{\max}$ is also very close to z_3.

3. Results and Discussion

[17] We evaluated the new solutions, equations (10) and (11), in comparison with the existing solutions for three test cases of *Salvucci* [1993] as presented in Table 1. As expected, equation (10) gives *Warrick*'s [1988] solution exactly. Here we used 10,000 terms of the series for both equation (10) and Warrick's solution, although it was found that about 20 terms for the sand and 100 terms for the clay adequately yield the exact solution of the problem.

[18] The results shown in Figure 2 also indicate an excellent agreement between approximations of equation (11) and

Table 1. Brooks-Corey Parameters and Relative Evaporation Rate (r) of the Test Cases of *Salvucci* [1993][a]

	h_b (cm)	K_s (cm/day)	P	$r = e/K_s$
Sand-loam	25	293.76	11.88	0.0005
Silt-loam	45	29.38	5.64	0.005
Clay	90	2.94	3.30	0.05

[a]The parameter h_b is bubbling pressure head, K_s is saturated hydraulic conductivity and $P = 2 + 3\lambda$.

the exact solution. However, a small deviation is observed for the case of the clay which comes from the series approximations. As a comparison, this figure also includes *Salvucci*'s [1993] approximate solution (his equation (12)) for Gardner $K(h)$ function, equation (3), showing a deviation from the exact solution under the drier conditions in the case of the clay. Note that the exact solutions for Brooks-Corey

and its equivalent Gardner conductivity functions fall on each other for the coarser soils. Figure 2 demonstrates the improvement of our solution for the pressure head profile of very fine-textured soils such as clay especially for dry conditions. However, a disadvantage compared to Salvucci's solution is that our solution is not explicitly invertible to the forms of $h(z, e)$ and $e(z, h)$.

[19] Derivation of equation (11) from equation (10) requires P being much larger than 1. Hence, the approximation errors will increase when P decreases. To evaluate the impact of P on the accuracy of equation (11), we studied the clay soil of Table 1 by decreasing its P down to 1. Results for three values of $P = 1.5$, 1.3, and 1.1 are shown in Figure 3. Approximation errors increase as P approaches 1 such that equation (11) entirely diverges from the exact solution when P gets 1.1 or smaller.

[20] We also applied equation (13) and (15) to predict D_{max} for the experimental data of *Gardner and Fireman*
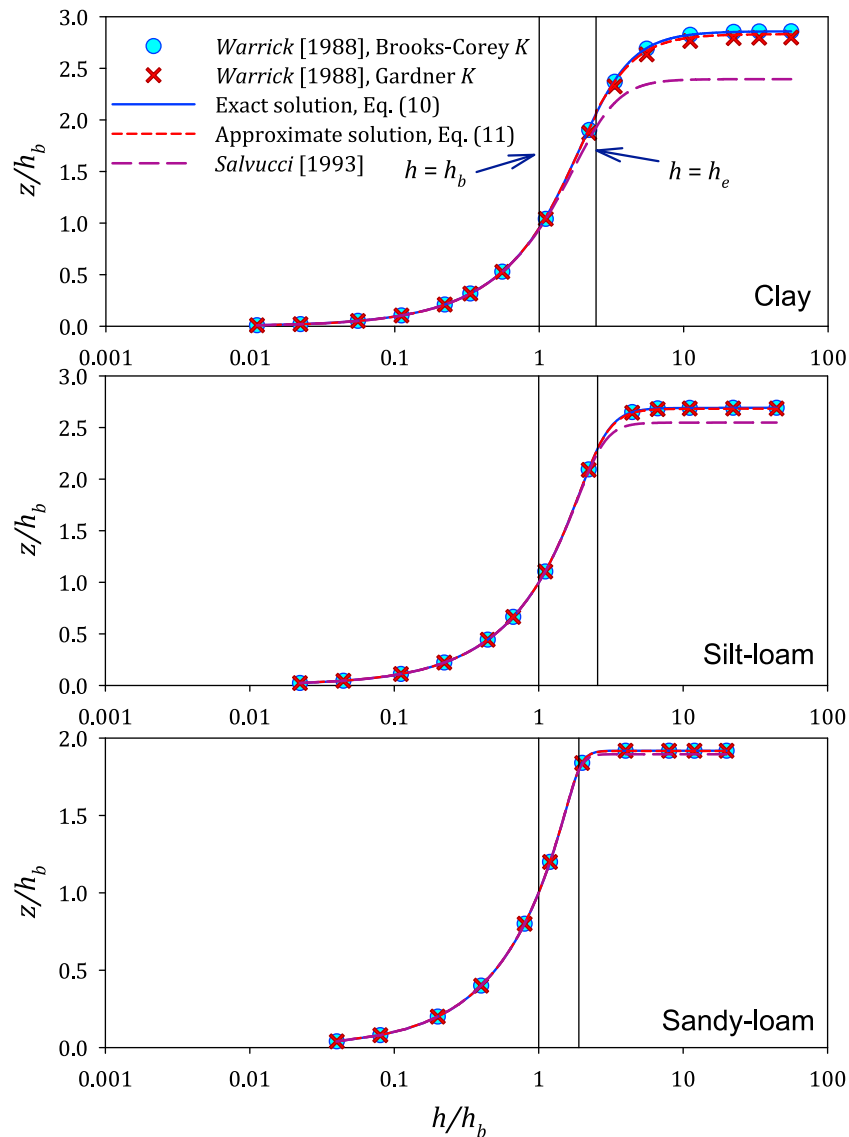

Figure 2. Comparison of the exact and approximate solutions of the pressure head profile above the water table during steady state evaporation for clay (P = 3.30), silt-loam (P = 5.64), and sandy-loam (P = 11.88) described in Table 1.
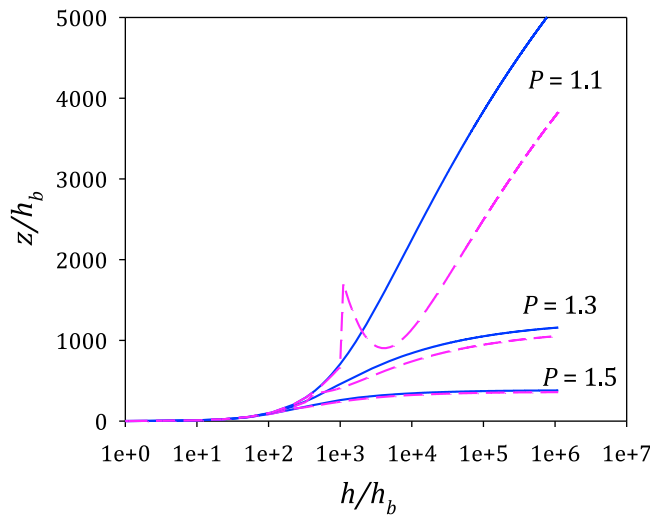
Figure 3. Comparison of the approximate solution, equation (11) (dashed line), with the exact solution (equation (10), solid line) for the clay soil in Table 1. As P approaches 1, the approximation fails due to the assumption used in the solution derivation that $P \gg 1$.

[1958], *Yang and Yanful* [2002], and *Shokri and Salvucci* [2011]. The hydraulic properties as well as the potential evaporative demand, e_0, used here are listed in Table 2.

[21] For the soils of *Gardner and Fireman* [1958], parameters of the Gardner model, equation (3), were reported. According to Figure 2, showing similar solution results for the Gardner and Brooks-Corey models, we used the same values for Brooks-Corey parameters. Since e_0 in their study was not reported, following *Shokri and Salvucci* [2011], we assumed that e_0 is the same as the evaporation rate at the shallowest water table applied ($D = 50$ and 60 cm for the Chino and Pachappa soils, respectively). For the soils of *Shokri and Salvucci* [2011], K_s was given and h_b and λ were obtained by fitting the Brooks-Corey retention model to the retention data reported, where λ is the power of the retention model. Then, P was estimated by the commonly accepted relationship of $P = 2 + 3\lambda$. For the soils of *Yang and Yanful* [2002], the same procedure was applied to the retention data reported in *Yanful et al.* [2003].

[22] Applying $e = e_0$ to equation (13) (or equation (15) in the case of the silt), values of $D_{\max}$ were obtained as presented in Figure 4. The figure shows the results in compari-

son with the results of the exact solution, equation (10), where an excellent agreement is found.

[23] Figure 5 shows the experimental data for evaporation rate scaled by e_0 as a function of scaled water table depth, $D/D_{\max}$. The figure generally indicates that e remains relatively high when D is smaller than $D_{\max}$. As soon as D becomes greater than $D_{\max}$, e significantly decreases due to the hydraulic disruption between the WT and soil surface. Figure 5 is similar to Figure 8 of *Shokri and Salvucci* [2011]. Comparing these two figures shows an improvement in the prediction of $D_{\max}$ for the Chino clay and Pachappa fine sandy loam soil, while the results for the other (coarser-textured) soils are very similar. The detachment of the scaled data of the Chino clay from those of the other soils may be attributed to the lower e_0 applied to this case (i.e., the adopted assumption of $e = e_0$ at $D = 50$ cm), while the other data show a reduction in evaporation rate when the WT is below the surface.

[24] We also learned that the solutions of Darcy's law (whether ours or other existing solutions) are somehow sensitive to the hydraulic parameters which always have some degree of uncertainty. To study this sensitivity for the Chino-, the silt-, and 1.02 mm-soil, we generated 1,000 random data sets from uniformly distributed values of h_b, K_s, and P between 80% and 120% of the respective parameters presented in Table 2. Using equation (13) and (15), $D_{\max}$ values were obtained between 30.45 and 104.94 cm for the Chino, 70.27 and 129.05 cm for the silt, and 8.58 and 15.39 cm for the 1.02 mm soil. As seen, the values are widely distributed especially for finer-textured soils. We found that the solution for finer-textured soils is sensitive to the change of all parameters, while not so sensitive for coarser-textured soils to parameters K_s and P. Therefore we conclude that a good prediction of $D_{\max}$ or other features of the evaporation process relies on an accurate determination of the hydraulic parameters.

4. Conclusions

[25] A novel exact solution to Darcy's law has been developed for a steady state evaporation process using the Brooks-Corey hydraulic conductivity model. The solution is presented in terms of a set of infinite series and can be reduced to a closed-form solution sufficiently accurate to describe a wide range of soil textures from sand to clay. The solution provides a simple tool to model the pressure head distribution above the water table as well as the maximum height of liquid continuity above the water table. The solution may also be used for directly modeling steady state

Table 2. Brooks-Corey Modeled Soil Parameters Used in This Study[a]

Soil Name	Reference	h_b (cm)	K_s (cm/day)	P	e_0 (cm/day)
Chino (clay)	*Gardner and Fireman* [1958]	23.77	1.95	2.00	0.80
Pachappa (fine sandy loam)	*Gardner and Fireman* [1958]	63.83	12.31	3.00	0.96
1.02 mm (quartz sand)	*Shokri and Salvucci* [2011]	7.17	280.0	12.68	0.99
0.48 mm (quartz sand)	*Shokri and Salvucci* [2011]	15.15	540.0	20.00	1.36
0.16 mm (quartz sand)	*Shokri and Salvucci* [2011]	32.26	650.0	36.89	0.67
Coarse sand	*Yang and Yanful* [2002]	4.92	63072	13.28	1.50
Fine sand	*Yang and Yanful* [2002]	34.84	1641	13.11	1.79
Silt	*Yang and Yanful* [2002]	151.51	1.64	5.62	1.73

[a]The parameter h_b is bubbling pressure head, K_s is saturated hydraulic conductivity, $P = 2 + 3\lambda$ and e_0 is the potential evaporative demand. For quartz sand, the numbers indicate the average particle size.
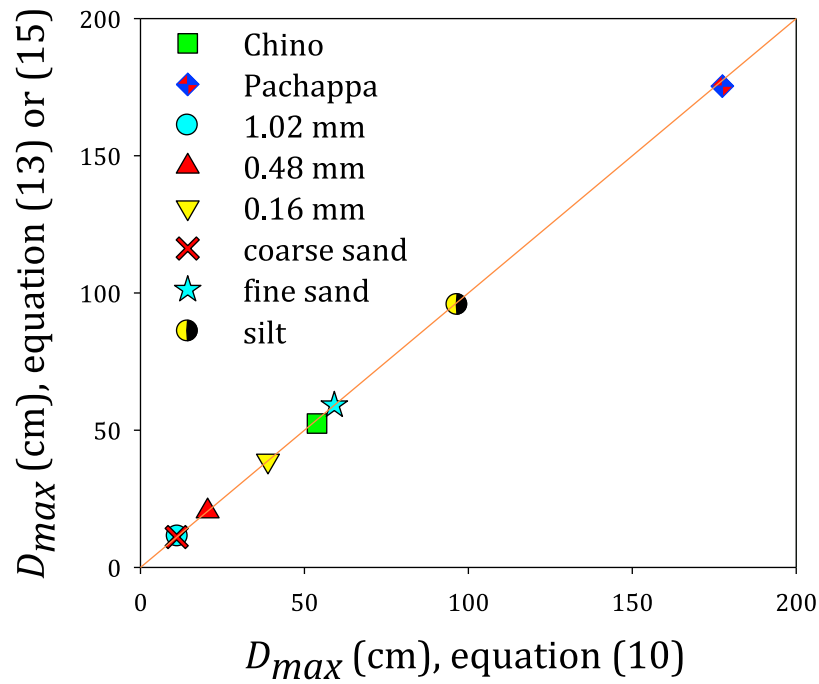
Figure 4. Maximum height of liquid continuity above the water table, D_{max}, calculated by equation (13) or (15) in comparison with the results of equation (10).
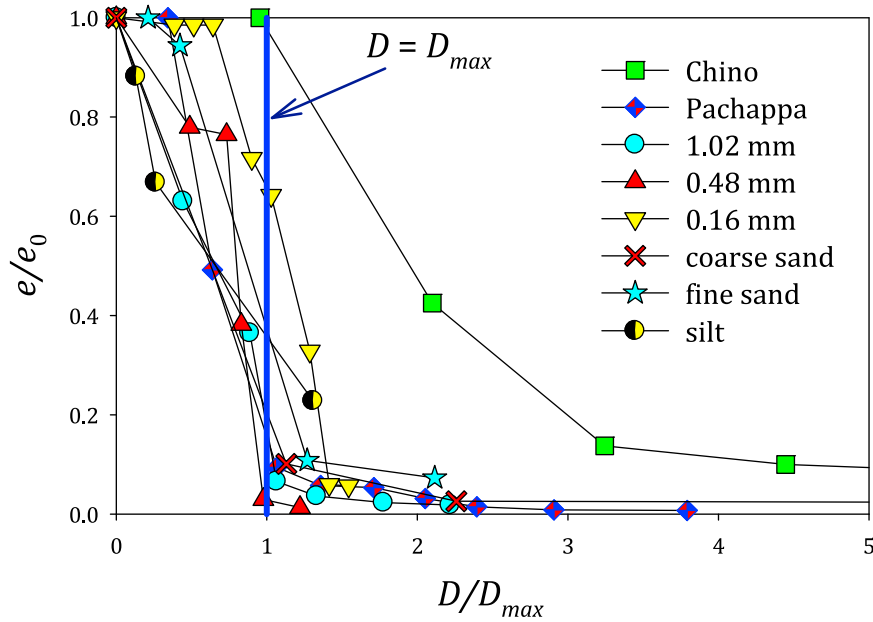

Figure 5. Experimental data (see Table 2) for steady state evaporation rate, e, as a function of water table depth, D. Data are scaled by the potential evaporative demand, e_0, and the maximum height of liquid continuity above the water table, D_{max}, calculated by equation (13) or (15).

evaporation or for inverse determination of the Brooks-Corey hydraulic conductivity parameters.

Appendix A: Derivation of Equation (11)

[26] Consider the first series in equation (10):

$$\sigma_1 = \sum_{i=0}^{\infty} \frac{(-1)^i (h/h_e)^{1+iP}}{1+iP} = \frac{h}{h_e} - \frac{(h/h_e)^{1+P}}{1+P}$$
$$+ \frac{(h/h_e)^{1+2P}}{1+2P} - \frac{(h/h_e)^{1+3P}}{1+3P} + \ldots \qquad (A1)$$

[27] Defining $x = (h/h_e)^P$, (A1) gives:

$$\sigma_1 = \frac{h}{h_e} - \frac{(h/h_e)}{1+P}\left[x - x^2\frac{1+P}{1+2P} + x^3\frac{1+P}{1+3P} + \ldots\right] \qquad (A2)$$

[28] For most soils, $P \gg 1$ and x^i (for $i \geq 2$) is very small when $|x| < 1$. (Since a boundary point does not contribute to an integrals' solution, the point $x = 1$ or $h = h_e$ can be excluded here.) Hence, considering $\ln(1 + x) = x - x^2/2 + x^3/3 + \ldots$ for $|x| < 1$, (A2) is closely approximated as follows:

$$\sigma_1 = \frac{h}{h_e} - \frac{(h/h_e)}{1+P}\left[x - \frac{x^2}{2} + \frac{x^3}{3} + \ldots\right]$$
$$= \frac{h}{h_e} - \frac{(h/h_e)}{1+P}\ln(1+x) = \frac{h}{h_e} - \frac{(h/h_e)}{1+P}\ln\left[1 + (h/h_e)^P\right] \quad (A3)$$

[29] In a similar way, it can be shown that:

$$\sigma_2 = \sum_{i=0}^{\infty} \frac{(-1)^i (h_b/h_e)^{1+iP}}{1+iP} = \frac{h_b}{h_e} - \frac{(h_b/h_e)}{1+P}\ln\left[1 + (h_b/h_e)^P\right] \qquad (A4)$$

and

$$\sigma_3 = \sum_{i=1}^{\infty} \frac{(-1)^{i+1}(h/h_e)^{1-iP}}{1-iP} = \frac{(h/h_e)}{1-P}\ln\left[1 + (h/h_e)^{-P}\right] \qquad (A5)$$

[30] Since the remaining series, σ_4, converges more slowly than the other series, we approximate it more carefully as follows:

$$\sigma_4 = \sum_{i=1}^{\infty} \frac{(-1)^{i+1}}{1-iP} = \frac{1}{1-P} - \frac{1}{1-2P} + \frac{1}{1-3P} - \ldots$$
$$= \frac{1}{1-P}\left(1 - \frac{1-P}{1-2P} + \frac{1-P}{1-3P} - \ldots\right)$$
$$= \frac{1}{1-P}\left(1 - \frac{1/2-P}{1-2P} - \frac{1/2}{1-2P} + \frac{1/3-P}{1-3P} + \frac{2/3}{1-3P} - \ldots\right)$$
$$= \frac{1}{1-P}\left(1 - \frac{1}{2} + \frac{1}{3} + \ldots\right) - \frac{1}{1-P}\left(\sum_{i=1}^{\infty} \frac{(-1)^{i+1}i}{(i+1)[1-(i+1)P]}\right) \qquad (A6)$$

[31] Assuming that $(i + 1)P \gg 1$ (for $i \geq 1$), the series appearing in equation (A6) can be approximated as follows [*Gradshteyn and Ryzhik*, 2000]:

$$\sum_{i=1}^{\infty} \frac{(-1)^{i+1}i}{(i+1)[1-(i+1)P]} = \frac{1}{-P}\sum_{i=1}^{\infty} \frac{(-1)^{i+1}i}{(i+1)^2} = \frac{-1}{P}\left(\frac{\pi^2}{12} - \ln 2\right) \qquad (A7)$$

[32] Which, in combination with (A6) yields:

$$\sigma_4 = \frac{\ln 2}{1-P} + \frac{\pi^2/12 - \ln 2}{P(1-P)} \qquad (A8)$$

[33] Substituting equations (A3), (A4), (A5), and (A8) into equation (10) yields equation (11).

References

Brooks, R. H., and A. T. Corey (1964), *Hydraulic Properties of Porous Media, Hydrol. Pap. 3*, Colorado State Univ., Fort Collins, Colo.

Edelfsen, N. E., and A. B. C. Anderson (1943), The thermodynamics of soil moisture, *Hilgardia*, 16, 31–298.

Gardner, W. R. (1958), Some steady state solutions of the unsaturated moisture flow equation with application to evaporation from a water table, *Soil Sci.*, 85, 228–232, doi:10.1097/00010694-195804000-00006.

Gardner, W. R., and M. Fireman (1958), Laboratory studies of evaporation from soil columns in the presence of a water table, *Soil Sci.*, 85, 244–249, doi:10.1097/00010694-195805000-00002.

Gowing, J. W., F. Konukcu, and D. A. Rose (2006), Evaporative flux from a shallow watertable: The influence of a vapour–liquid phase transition, *J. Hydrol.*, 321(1–4), 77–89, doi:10.1016/j.jhydrol.2005.07.035.

Gradshteyn, I. S., and I. M. Ryzhik (2000), *Table of Integrals, Series, and Products*, 6th ed., Academic, San Diego, Calif.

Lehmann, P., S. Assouline, and D. Or (2008), Characteristic lengths affecting evaporative drying of porous media, *Phys. Rev. E*, 77(5), 056309, doi:10.1103/PhysRevE.77.056309.

Salvucci, G. D. (1993), An approximate solution for steady vertical flux of moisture through an unsaturated homogeneous soil, *Water Resour. Res.*, 29(11), 3749–3753, doi:10.1029/93WR02068.

Shokri, N., and G. D. Salvucci (2011), Evaporation from porous media in the presence of a water table, *Vadose Zone J.*, 10(4), 1309–1318, doi:10.2136/vzj2011.0027.

Shokri, N., P. Lehmann, and D. Or (2009), Critical evaluation of enhancement factors for vapor transport through unsaturated porous media, *Water Resour. Res.*, 45, W10433, doi:10.1029/2009WR007769.

Warrick, A. W. (1988), Additional solutions for steady-state evaporation from a shallow water table, *Soil Sci.*, 146, 63–66, doi:10.1097/00010694-198808000-00001.

Yanful, E. K., S. Morteza Mousavi, and M. Yang (2003), Modeling and measurement of evaporation in moisture-retaining soil covers, *Adv. Environ. Res.*, 7(4), 783–801, doi:10.1016/S1093-0191(02)00053-9.

Yang, M., and E. K. Yanful (2002), Water balance during evaporation and drainage in cover soils under different water table conditions, *Adv. Environ. Res.*, 6(4), 505–521, doi:10.1016/S1093-0191(01)00077-6.

Yiotis, A. G., A. G. Boudouvis, A. K. Stubos, I. N. Tsimpanogiannis, and Y. C. Yortsos (2003), Effect of liquid films on the isothermal drying of porous media, *Phys. Rev. E*, 68(3), 037303, doi:10.1103/PhysRevE.68.037303.